Multiple mitochondrial thioesterases have distinct tissue and substrate specificity and CoA regulation, suggesting unique functional roles

Received for publication, September 3, 2019, and in revised form, October 16, 2019 Published, Papers in Press, November 1, 2019, DOI 10.1074/jbc.RA119.010901

Carmen Bekeova[‡], Lauren Anderson-Pullinger[‡], Kevin Boye[‡], Felix Boos[§], Yana Sharpadskaya[‡], Johannes M. Herrmann[§], and Erin L. Seifert[‡1]

From the [‡]MitoCare Center, Department of Pathology, Anatomy, and Cell Biology, Thomas Jefferson University, Philadelphia, Pennsylvania 19107 and the [§]Division of Cellular Biology, Department of Biology, University of Kaiserslautern, 67663 Kaiserslautern, Germany

Edited by Jeffrey E. Pessin

Acyl-CoA thioesterases (Acots) hydrolyze fatty acyl-CoA esters. Acots in the mitochondrial matrix are poised to mitigate β-oxidation overload and maintain CoA availability. Several Acots associate with mitochondria, but whether they all localize to the matrix, are redundant, or have different roles is unresolved. Here, we compared the suborganellar localization, activity, expression, and regulation among mitochondrial Acots (Acot2, -7, -9, and -13) in mitochondria from multiple mouse tissues and from a model of Acot2 depletion. Acot7, -9, and -13 localized to the matrix, joining Acot2 that was previously shown to localize there. Mitochondria from heart, skeletal muscle, brown adipose tissue, and kidney robustly expressed Acot2, -9, and -13; Acot9 levels were substantially higher in brown adipose tissue and kidney mitochondria, as was activity for C4:0-CoA, a unique Acot9 substrate. In all tissues, Acot2 accounted for about half of the thioesterase activity for C14:0-CoA and C16:0-CoA. In contrast, liver mitochondria from fed and fasted mice expressed little Acot activity, which was confined to long-chain CoAs and due mainly to Acot7 and Acot13 activities. Matrix Acots occupied different functional niches, based on substrate specificity (Acot9 *versus* Acot2 and -13) and strong CoA inhibition (Acot7, -9, and -13, but not Acot2). Interpreted in the context of β-oxidation, CoA inhibition would prevent Acot-mediated suppression of β-oxidation, while providing a release valve when CoA is limiting. In contrast, CoA-insensitive Acot2 could provide a constitutive siphon for long-chain fatty acyl-CoAs. These results reveal how the family of matrix Acots can mitigate β-oxidation overload and prevent CoA limitation.

This work was supported by American Heart Association Grant 13SDG14380008, National Institutes of Health Grant R01 DK109100 (to E. L. S.), and Thomas Jefferson University start-up funds (to E. L. S.). The authors declare that they have no conflicts of interest with the contents of this article. The content is solely the responsibility of the authors and does not necessarily represent the official views of the National Institutes of Health.

This article contains supporting information.

[1] To whom correspondence should be addressed: MitoCare Center, Dept. of Pathology, Anatomy, and Cell Biology, Suite 527 JAH, Thomas Jefferson University, Philadelphia, PA 19107. Tel.: 215-503-5030; Fax: 215-923-2218; E-mail: erin.seifert@jefferson.edu.

Acyl-CoA thioesterases (Acots)[2] hydrolyze acyl-CoA into CoA and an acyl chain and are classified into two families based on functional domain. Type I Acots are members of the superfamily of α/β-hydrolases, are found only in mammals, and have a high degree of similarity (1). Humans and rodents possess Type I Acots residing within the cytoplasm (Acot1), mitochondria (Acot2), and peroxisomes (Acot3–6 in rodents, Acot3–4 in humans) (1). In contrast, Type II Acots (Acot7–15) share little similarity beyond a hotdog fold domain (2). Some possess StAR-related lipid transfer domains (2) or can interact with a Start domain protein (3) and are found in the cytoplasm (Acot7–14), mitochondria (Acot7–13 and Acot15), and peroxisomes (Acot8) (2). Dual localization is also possible (Acot7, -11, and -13). Type I and II Acots have a signature substrate specificity that includes saturated and unsaturated fatty acyl-CoAs of different chain lengths and, in fewer cases, other CoA esters (3–5).

Acots are predicted to have high biological relevance because their substrates, acyl-CoA esters, are also substrates for other enzymes that serve major metabolic pathways, such as mitochondrial β-oxidation, and can serve as allosteric or covalent regulators. In fact, genetic manipulation in mice of Type I or II Acots is associated with altered phenotypes (2, 7, 8). For example, mice with whole-body Acot13 deletion had improved glucose homeostasis on a high-fat diet (9) and improved hepatic insulin sensitivity in the setting of steatosis (10). Although these observations suggest that Acot13 loss protects fatty liver from insulin resistance, it should be noted that Acot13 has dual mitochondria-cytosol localization and that the subcompartmentalization of Acot13 within mitochondria has not yet been determined. Thus, it remains unclear whether the response to Acot13 loss primarily reflects an effect of cytosolic or mitochondrial Acot13 loss.

Despite the availability of genetic mouse models and information about the Acots, there are basic unexplored questions,

[2] The abbreviations used are: Acot, acyl-CoA thioesterase; BAT, brown adipose tissue; MTS, mitochondrial targeting sequence; OMM, outer mitochondrial membrane; IMM, inner mitochondrial membrane; IMS, intermembrane space; PDH, pyruvate dehydrogenase; Cyto *c*, cytochrome *c*; PPAR, peroxisomal proliferator-activated receptor; MCKAT, medium-chain ketoacyl-CoA thiolase; SDHA, succinate dehydrogenase; ANOVA, analysis of variance.

the answers to which should help provide mechanistic insights into how Acots alter phenotypes and how to interpret models of Acot depletion. A fundamental question is whether the Acots within a cellular compartment occupy functional or tissue-specific niches or whether, instead, different Acots are largely redundant, with distinction only in substrate specificity; whether this is the case has not been considered. Therefore, to investigate this question, we focused on Acots associated with mitochondria: Acot2, -7, -9, -11, -13, and -15. In particular, what is not clear is total Acot activity within mitochondria of different tissues, the substrate specificity of this activity, and the mitochondrial Acots that contribute to it in a tissue-specific manner. Also, the subcompartmentalization within mitochondria is not known for all of the Acots, Finally, regulation is incompletely understood.

We addressed these questions by evaluating the suborganellar localization of Acot7, -9, and -13. Then, to evaluate tissue and substrate specificity, we compared four mitochondrial thioesterases (Acot2, -7, -9, and -13) in terms of activity and expression, using five mouse tissues. To compare among these Acots in terms of regulation by metabolic stimuli, effects on their expression and activity of fasting and potential allosteric regulators were evaluated in mitochondria from mouse tissues and recombinant enzymes. A new mouse model of Acot2 depletion allowed us to estimate the quantitative contribution of Acot2 and Acot13 toward the thioesterase activity for long-chain fatty acyl-CoA esters. Altogether these data reveal distinct functional roles for four mitochondrial Acots.

Results

Localization of Acot7, -9, and -13 to the mitochondrial matrix

Subcompartmental localization of Acot2 and Acot15 to the mitochondrial matrix was demonstrated by immunogold EM (11, 12), whereas localization of Acot7, -9, and -13 within mitochondria has not been determined. Acot7 and -9 each express an N-terminal mitochondrial targeting sequence (MTS) with high probability (84 or 93% for Acot7, depending on isoform (see below); 93% for Acot9; MTS predictions from TargetP). Acot13, with only a weak TargetP score (30%), has been suggested to reside on the outer surface of the outer mitochondrial membrane (OMM) (2), but this has not been demonstrated. Acot11, with only a low-probability MTS, was previously found localized to the matrix of HEK293T cells (13). Thus, we determined its mitochondrial localization in mouse tissues. We used a protease protection approach to analyze the subcompartmentalization of Acot7, -9, and -13. Proteolytic destabilization of the protein following strong membrane disruption by Triton X-100 served as a positive control. Validated antibodies specifically targeting Tom20, Tim23, and pyruvate dehydrogenase (PDH) were used to mark the OMM, intermembrane space (IMS)/inner mitochondrial membrane (IMM), and matrix, respectively.

We first determined the specificity of the Acot13 antibody using recombinant Acot13 and liver mitochondria from Acot13 knockout mice (Fig. 1*A*). Control samples revealed a single band at ~15 kDa; bands near 15 kDa were not detected in the Acot13 knockout sample unless the membrane was overexposed, in which case faint bands were similar across the protease/detergent conditions (Fig. 1*A*, *right*). Thus, the anti-Acot13 antibody is specific for Acot13 in isolated mitochondria.

Next, we exposed isolated mitochondria from three tissues to two different proteases in the absence or presence of Triton X-100 or increasing digitonin and evaluated the expression of Tom20, Tim23, PDH, and Acot13. Tom20 was digested by protease alone, Tim23 usually required the addition of digitonin for digestion and was more susceptible to trypsin than to proteinase K, and PDH was only digested when Triton X-100 was added (Fig. 1, *A*, *B*, *E*, and *F*). In mitochondria from liver, kidney, and heart with either trypsin or proteinase K, Acot13 was only digested in the presence of Triton X-100 and thus followed the pattern of matrix-localized PDH (Fig. 1, *B* and *E*).

It was possible that some Acot13 was loosely associated with the outer surface of the OMM but was dislodged during tissue homogenization. We reasoned that if this occurred, the supernatant fraction of the high-speed spin used to pellet mitochondria would contain a substantial amount of Acot13. Indeed, Acot13 was previously found in the supernatant fraction, and it was concluded that it can reside in the cytoplasm as well as be associated with mitochondria (3). To estimate the fraction of Acot13 in the cytoplasm (or loosely bound to the OMM), immunoblot analysis was conducted on different fractions from the liver and heart mitochondria isolations (Fig. 1*C*). Compared with the amount of Acot13 detected in the total homogenate, ~5 times more was found in the high-speed pellet from liver and ~2 times more was found in the high-speed pellet from heart. In contrast, band intensity in the supernatant of both tissues was less than half of that in the total homogenate. For the heart, this pattern of distribution of Acot13 between pellet and supernatant was similar to that for three IMM proteins (Complex I 37-kDa subunit, Complex II SDHA subunit, Complex III Core I subunit), raising the possibility that, in the heart, Acot13 in the supernatant reflects co-contaminating mitochondrial proteins rather than a cytoplasmic or OMM-associated fraction.

The situation for the liver was different (Fig. 1*C*). Acot13 in the supernatant as a fraction of the total liver homogenate was substantially higher than that for any of the three IMM proteins (0.4 for Acot13 *versus* 0.1–0.2 for C-I, SDHA, and C-III), suggesting that, in the liver, some Acot13 was present in the cytoplasm and/or very loosely associated with the OMM. However, for both liver and heart, the majority of Acot13 was present in the high-speed pellet and thus would situate a substantial amount of Acot13 within the matrix.

Analysis using MTS prediction algorithms indicated an MTS probability of mouse Acot13 of ~30% (TargetP) or 39% (MitoProt II algorithm). MTS prediction for human Acot13 isoform 1 was higher (~52%, TargetP; 63%, MitoProt II) and was lower for human Acot13 isoform 2 (~12% using TargetP; 50%, MitoProt II). We searched for an internal targeting sequence (14) by sequentially shortening the amino acid sequence by 1 amino acid starting at the N-terminal; there was no MTS greater than 20% anywhere within the protein.

Perusing MitoCarta2.0 revealed *bona fide* matrix proteins having MTS predictions <30% (*e.g.* ribosomal proteins MRPS22, MRPL42, and MRPL48). This, together with matrix

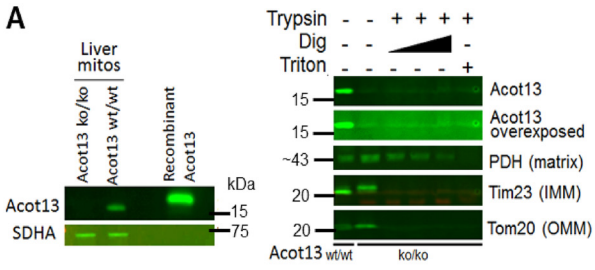

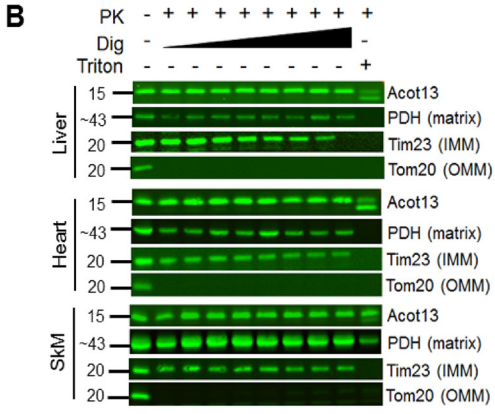

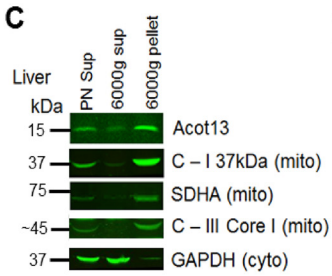

Quantified relative to PN Sup (PN Sup = 1, not shown):

Liver	7000g sup	7000g pellet
Acot13	0.4	5.3
C-I	0.14	17.8
SDHA	0.2	14.2
C-III	0.1	27.9
GAPDH	1.2	0.1

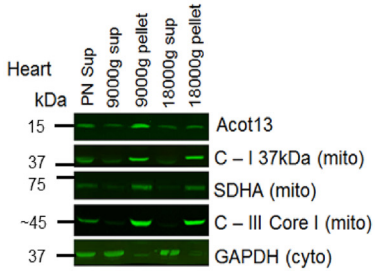

Quantified relative to PN Sup (=1, not shown):

Heart	9000g sup	9000g pellet	18000g sup	18000 pellet
Acot13	0.45	1.94	0.54	0.64
C-I	0.37	1.49	0.26	1.37
SDHA	0.43	2.0	0.24	1.55
C-III	0.2	3.0	0.08	2.7
GAPDH	1.1	1.2	1.24	0.16

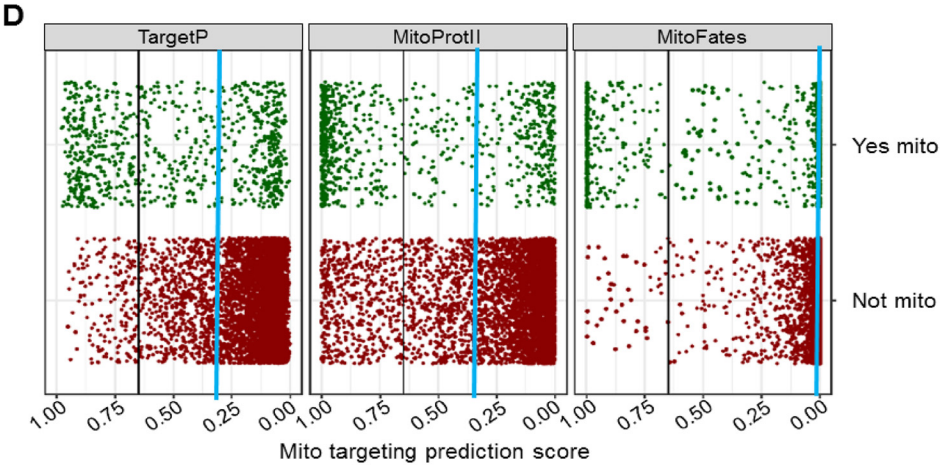

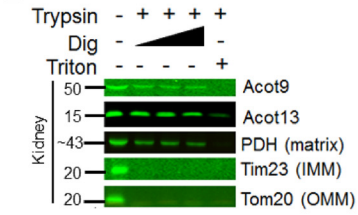

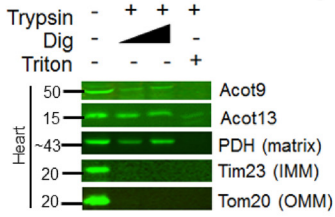

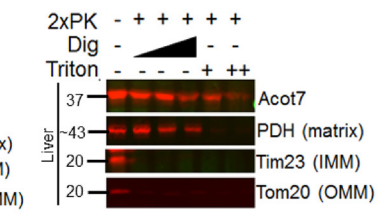

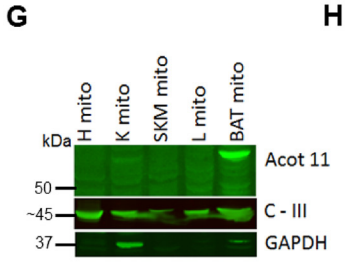

H

	MTS (TargetP)	MitoCarta 2.0	Mito location	Evidence	Dual location
Acot2	74%	Y	Matrix	Immuno-gold EM (ref. 8)	No
Acot7	Isoform 1: 84% Isoform 3: 93%	N	Matrix	Fractionation+protease protection: present study	Yes: mito and cytosol splice variants
Acot9	74%	Y	Matrix	Fractionation+protease protection: present study	No
Acot13	30%	Y	Matrix	Fractionation+protease protection: present study	Yes: mito and cytosol
Acot15	95%	N	Matrix	Immuno-gold EM (ref. 9)	No

localization of Acot13 despite its low MTS prediction score prompted us to systematically determine the reliability of MTS prediction algorithms using a recently published high-confidence mitochondrial yeast proteome (15). Using the TargetP, MitoFates, and MitoProt II algorithms and a cutoff MTS probability of 65%, the false negative rate (high-confidence mitochondrial proteins with MTS <65%) was 60, 56, and 38% for each algorithm, respectively. The false positive rate (high-confidence, nonmitochondrial protein with MTS >65%) was 4, 1, and 14% for each algorithm, respectively. Furthermore, plotting the MTS scores for high-confidence mitochondrial and nonmitochondrial proteins revealed many high-confidence mitochondrial proteins with MTS scores <25% (Fig. 1*D*). We also analyzed the human and mouse MitoCarta2.0 databases (16) for proteins annotated as "Apex_matrix"; ~6% of these proteins had a low MTS score (category "5" in MitoCarta) or were categorized as having no MTS ("no score" in MitoCarta). These analyses indicate that MTS scores >65% predict mitochondrial proteins well, whereas a low MTS score is unreliable as evidence that a protein is nonmitochondrial. This can, in part, occur as some mitochondrial proteins carry targeting signals other than a classical N-terminal MTS. Whereas these are characterized for some classes of proteins (*e.g.* substrates of TIM22 or MIA pathways), targeting information for many of these proteins is unknown.

Localization of Acot9 was tested in kidney and heart mitochondria, as it is robustly expressed (5) (Fig. 2). A custom antibody tested in mouse tissues (5) was used and shows a single band of ~50 kDa, with minimal or no additional bands. In both kidney and heart mitochondria, the 50 kDa band disappeared only after adding trypsin plus Triton X-100, as was found for matrix PDH (Fig. 1*E*).

Acot7 has three transcripts annotated in NCBI. Transcripts 1 and 3 have a strongly predicted MTS (84 and 93%, respectively, using TargetP), whereas prediction for transcript 2 is only 11%. The custom anti-Acot7 antibody was validated in tissues from Acot7 knockout mice (17). Using this antibody, we found that the predominant band is at ~37 kDa (cleaved N-terminal sequence in isoforms 1 and 3). Occasional faint bands appeared at ~42 kDa (representing the unprocessed protein) and ~50 kDa. We found that liver mitochondria clearly expresses the 37 kDa band, whereas signals were much weaker or barely detectable in mitochondria isolated from other tissues (see Fig. 2*A*). Thus, we selected only liver mitochondria for further protease experiments. The 37 kDa band recognized by the anti-Acot7 antibody was destabilized only when the sample was treated with protease plus Triton X-100 (Fig. 1*F*) and thus followed the same pattern as matrix-localized PDH.

Finally, using an antibody against Acot11 validated in knockout mouse tissue (18), a band was observed in the high-speed pellet fraction in the brown adipose tissue (BAT) preparation but not in the high-speed pellets from heart, skeletal muscle, liver, or kidney (Fig. 1*G*).

Fig. 1*H* summarizes the localization of the mitochondrial Acots empirically determined here and in previous studies.

Tissue-specific Acot expression and thioesterase activity

The above observations indicate that Acot13 joins Acot2, -7, -9, and -15 as Acots that localize to the matrix, raising the possibility of redundancy among the five mitochondrial Acots. Tissue-specific expression would be one way that these Acots are not redundant. Here we compared Acot protein expression and thioesterase activity among mitochondria from five tissues. Two of these, liver and heart, have already been associated with mitochondrial Acot expression (4, 19–23). Three other tissues, skeletal muscle, BAT, and kidney, are known to express mitochondrial Acots (5, 17, 22, 24, 25) but have been relatively less studied.

There were several methodological considerations for the immunoblotting studies. First, concerning the antibodies, those against Acot2, -7, and -13 have been tested in knockout mice (12, 17, 26) (this work), whereas there is no reliable commercially available antibody against Acot15. Second, mitochondrial fractions were largely devoid of cytoplasmic proteins (*e.g.* see Fig. 1*C*). Third, for normalization, samples were probed for three different proteins: the 37-kDa subunit of C-I, SDHA, and cytochrome *c* (Cyto *c*). The average of the normalized values was used. A new aliquot of the Acot2 antibody that was used for BAT mitochondria generated multiple bands; for interpretation, these immunoblots included samples from Acot2 whole-body knockout mice ($Acot2^{-/-}$; see Fig. 3*B*). BAT was excluded from the Acot7 analysis because the Acot7 antibody generated multiple bands centered around 37 kDa.

Heart, skeletal muscle, BAT, and kidney mitochondria all robustly expressed Acot2 and Acot13 (Fig. 2*A*). Skeletal muscle, BAT, and kidney mitochondria also expressed Acot9, and heart

Figure 1. Acot7, -9, and -13 localize to the mitochondrial matrix. Protease protection experiments (*A*, *B*, *E*, and *F*) determined the submitochondrial location of Acot7, -9, and -13 using trypsin or proteinase K (*PK*), and increasing digitonin (*Dig*) concentration. Triton X-100 plus protease served as a positive control for protease sensitivity. Tom20 marked the OMM, Tim23 marked the IMS/IMM, and PDH marked the matrix. In all *panels*, mitochondria were isolated from the indicated mouse tissue. *A*, recombinant Acot13 and liver mitochondria from Acot13 knockout (*ko/ko*) and WT (*wt*) mice were used to determine the specificity of the anti-Acot13 antibody. Note that the molecular weight of recombinant Acot13 is slightly higher than endogenous Acot13 due to the presence of a His_{10} tag on recombinant Acot13. *B*, protease protection experiment to determine the subcompartmentalization of Acot13, using the mitochondrial fraction of a liver fractionation. *C*, distribution of Acot13 between mitochondria (pellet) and nonmitochondrial fraction. Subunits of electron transport chain Complex I, II, and III (*C - I*, *SDHA*, and *C - III*) were used to mark mitochondria. Glyceraldehyde 3-phosphate dehydrogenase (*GADPH*) marked the cytoplasm. Values were calculated by expressing supernatant (*Sup*) and "pellet" as a fraction of the post-nuclear (*PN*) supernatant (*PN Sup = 1*, *not shown*). *D*, MTS prediction accuracy by three algorithms using data from a high-confidence mitochondrial proteome from yeast (15). Yeast proteins were classified as mitochondrial (*Yes mito*) or nonmitochondrial (*Not mito*) according to Ref. 15. The amino acid sequences of the complete proteome of reference strain S288C were retrieved from the Saccharomyces Genome Database and subjected to MTS prediction using the TargetP, MitoProt II, and MitoFates algorithms. The resulting prediction scores for mitochondrial localization are plotted as points for each individual protein. *Blue lines* mark the MTS prediction for Acot13. *E* and *F*, protease protection experiment to determine the subcompartmentalization of Acot9 (*E*) and Acot7 (*F*) using the mitochondrial fraction of kidney, heart, and liver fractionations. *G*, Acot11 is not widely expressed in mitochondria from various tissues. *H*, heart; *K*, kidney; *SKM*, skeletal muscle; *L*, liver. *H*, summary of mitochondrial Acots, likelihood of an MTS (calculated using TargetP algorithm), whether or not the Acot is annotated in MitoCarta 2.0 (16) as a mitochondrial protein, the evidence for localization within mitochondria, and whether or not the Acot is dual-localized. *A*, *B*, *C*, *E*, *F*, and *G*, amounts loaded are 5 μg of mitochondria to detect Acot13, 30 μg of mitochondria to detect Acot9, 20 μg of mitochondria to detect Acot7, and 10 ng of recombinant Acot13

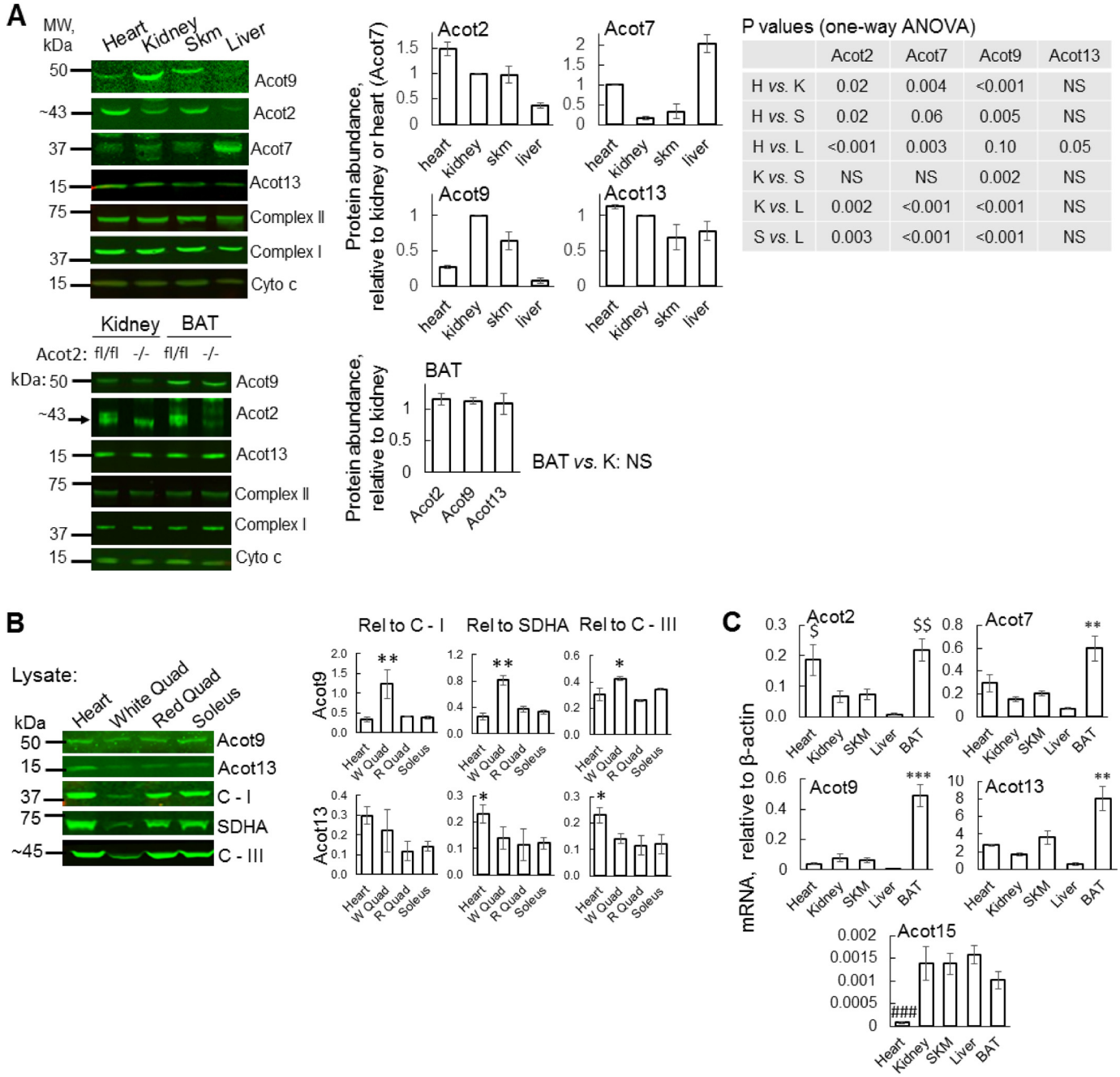

Figure 2. Tissue-specific localization of mitochondrial Acots. *A*, immunoblot analysis using isolated mitochondria. For the quantification, normalization was to Complex I, Complex II (SDHA), and Cyto *c*; normalizations to each of the latter were averaged and then expressed relative to that for kidney or heart mitochondria (equal to 1.0). The *table* shows *p* values, one-way ANOVA, and Tukey post hoc tests. *H*, heart mitochondria; *K*, kidney mitochondria; *S*, skeletal muscle mitochondria; *L*, liver mitochondria; *NS*, not significant. The antibody against Acot2 used with the BAT samples yielded nonspecific bands slightly below the Acot2 band. To interpret the Acot2 bands, mitochondria from Acot2$^{-/-}$ tissues were run in parallel. Only the upper band (*arrow*) of the WT samples was used for quantification. The Acot7 signal was not evaluated in BAT because the antibody yielded many nonspecific bands. Values are mean ± S.E. (*error bars*), $n = 5–6$. The amount of protein loaded was 30 μg for Acot2 and Acot9, 40 μg for Acot7, 5 μg for Acot13, Complex I, SDHA, and Cyto *c*. *B*, immunoblot analysis using muscle lysates (40 μg). The quantification shows mean ± S.E. (*error bars*), $n = 3$, Acot values expressed relative to different abundant mitochondrial proteins (Complex I, SDHA, or Complex III). Statistical analysis was by one-way ANOVA and Tukey post hoc pairwise comparisons (*p* values refer to Tukey test): * and **, $p = 0.01$ and 0.05, respectively, *versus* all other muscles. *C*, mRNA expression by quantitative PCR. Values are mean ± S.E., $n = 5–6$. Statistical analysis was by one-way ANOVA and Tukey post hoc pairwise comparisons (*p* values refer to Tukey test): $, $p = 0.05$, heart *versus* kidney, skeletal muscle (*Skm*), and liver; $$, $p = 0.01$ BAT *versus* kidney, skeletal muscle, and liver; *** and **, $p < 0.001$ and $p = 0.003$, respectively, BAT *versus* all other tissues; ###, $p < 0.001$, heart *versus* all other tissues.

did as well but at a level that was 40–50% of the activity in the other tissues. Acot7 was low in mitochondria from these tissues. Liver mitochondria expressed Acot7 and Acot13, but very little Acot2 and Acot9. Thus, mitochondria from skeletal muscle, BAT, kidney, and heart robustly expressed three different matrix Acots (Acot2, Acot9, and Acot13), whereas liver mitochondria show lower Acot expression, mainly contributed by Acot13 and Acot7.

Glycolytic and oxidative muscles express a different abundance of proteins mediating metabolism and signaling, includ-

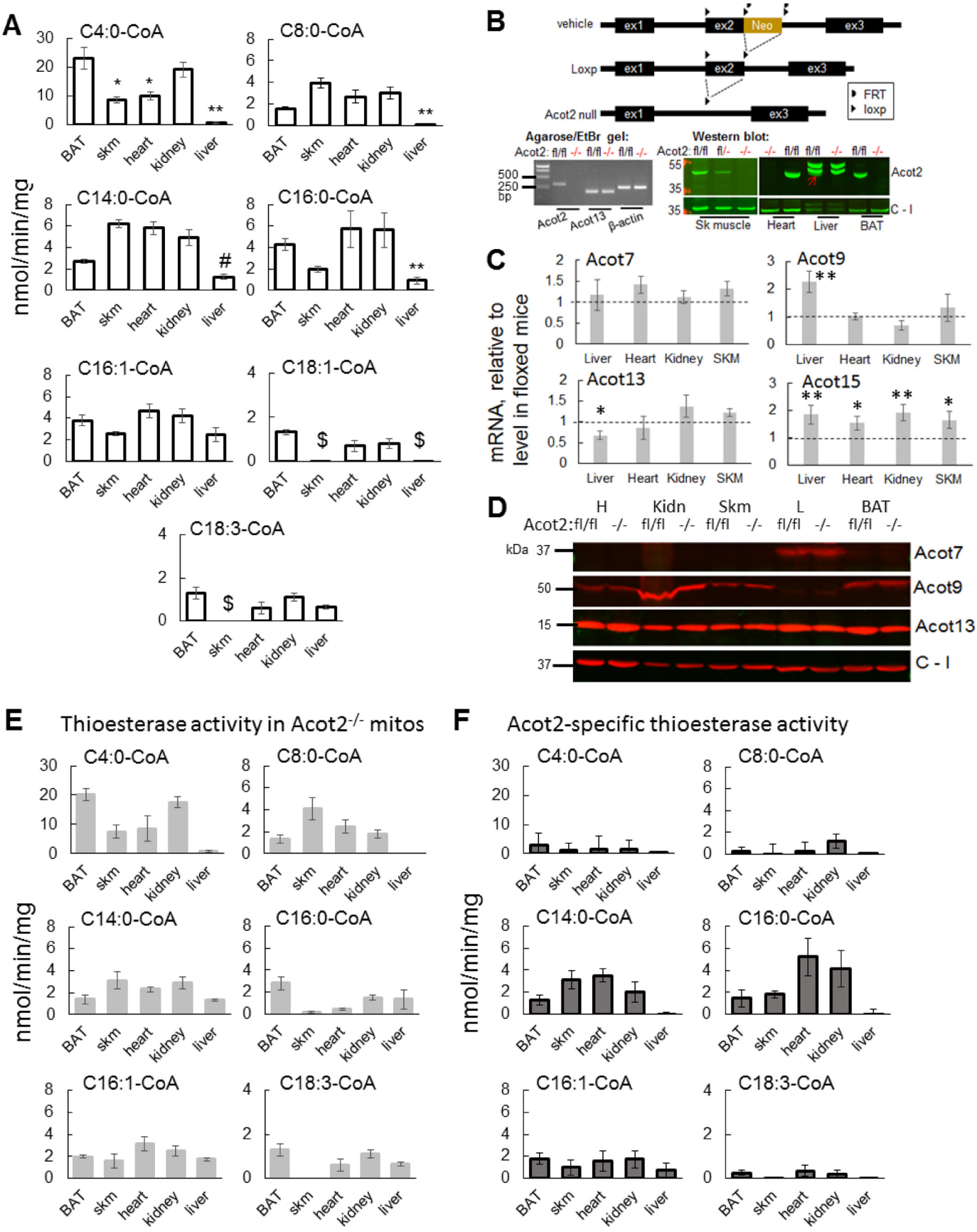
A
C4:0-CoA
C8:0-CoA
C14:0-CoA
C16:0-CoA
C16:1-CoA
C18:1-CoA
C18:3-CoA
nmol/min/mg
BAT
skm
heart
kidney
liver
B
vehicle
Loxp
Acot2 null
ex1
ex2
Neo
ex3
FRT
loxp
Agarose/EtBr gel:
Western blot:
Acot2
Acot13
β-actin
Sk muscle
Heart
Liver
BAT
C - I
C
mRNA, relative to level in floxed mice
Acot7
Acot9
Acot13
Acot15
Liver
Heart
Kidney
SKM
D
H
Kidn
Skm
L
BAT
kDa
E
Thioesterase activity in Acot2-/- mitos
F
Acot2-specific thioesterase activity

ing proteins encoded by peroxisomal proliferator-activated receptor (PPAR)-induced genes. Because some Acots are induced by PPAR agonists (3, 11, 19, 21, 22, 27–29), we tested mitochondrial Acot expression in different skeletal muscles, namely in soleus (highly oxidative), white quadriceps (glycolytic), and the redder portion of gastrocnemius (mixed oxidative). Lysates were used because mitochondria cannot be reliably isolated from small pieces of mouse skeletal muscle. Because the Acot2 antibody likely also recognizes cytoplasmic Acot1, and showed multiple bands in muscle lysates, Acot abundance in different muscles was determined for Acot9 and Acot13 but not Acot2. Acot9 showed relatively higher expression in white gastrocnemius compared with oxidative muscles and heart (Fig. 2*B*). In contrast, Acot13 expression was similar in glycolytic and oxidative muscles (Fig. 2*B*).

Although a tissue comparison of Acot mRNA was recently published (17), as a complement to our data set, we evaluated mRNA levels in the five tissues studied here (Fig. 2*C*). Data generally agree with published values. Notably, Acot2, Acot7, and Acot13 mRNA were robust in all tissues except the liver.

To further understand the relative contribution of different matrix Acots to a tissue's thioesterase activity, we measured thioesterase activity using a range of acyl-CoA species that covers the substrate specificity of the matrix Acots. Activity measurements also allow quantitative comparisons among substrates within a tissue.

Thioesterase activity for C4:0-CoA was by far the highest, at 10–20 nmol/min/mg *versus* 1–6 nmol/min/mg for the other substrates (Fig. 3*A*) (in all cases, unless otherwise stated, mg refers to mg of mitochondrial protein). BAT and kidney mitochondria showed the highest activity for C4:0-CoA (~20 nmol/min/mg), followed by heart and skeletal muscle mitochondria (~10 nmol/min/mg). Activity toward C4:0 was very low in liver mitochondria. This pattern of activity for C4:0-CoA is consistent with the Acot9 protein abundance in these tissues and the fact that the only Acot known to show activity for C4:0-CoA is Acot9 (3, 5, 12, 30).

Thioesterase activity for C8:0-CoA was lower (2–4 nmol/min/mg) than for C4:0-CoA but showed a similar tissue distribution as for C4:0, including minimal activity in liver mitochondria (Fig. 3*A*). As for C4:0-CoA, C8:0-CoA is a good substrate for Acot9 (5) but not Acot2, -13, or -15 (3, 11, 12). Thus, thioesterase activity toward C4:0- and C8:0-CoA can be used as a surrogate for Acot9 expression in BAT, kidney, heart, and skeletal muscle.

Thioesterase activity for C14:0-, C16:0-, and C16:1-CoA was 2–6 nmol/min/mg in mitochondria from all tissues, with activity in liver mitochondria at the lower end of the range and in heart at the higher end (Fig. 3*A*). This pattern of activity among tissues generally matched protein levels for Acot2 and Acot13, which both have C14:0-, C16:0-, and C16:1-CoA as major substrates. Acot9 is reported to have substantial activity for C14:0-CoA (but not for C16:0- or C16:1-CoA) (5). However, activity for C14:0-CoA was not higher in BAT and kidney mitochondria, which expressed the most Acot9. Similarly, C14:0- and C16:0-CoA are good substrates for Acot7 (30), yet liver mitochondria, with the most Acot7 among the five tissues, had low activity toward these substrates. Thus, Acot7 and Acot9 may have different substrate selectivity in their native context.

Finally, we tested thioesterase activity toward C18:1-CoA and C18:3-CoA, major substrates for Acot15 but poor substrates for the other mitochondrial Acots (5, 12, 28, 30). In mitochondria from all tissues, activity for either substrate was ~1 nmol/min/mg (Fig. 3*A*). Thus, the contribution of Acot15 to matrix thioesterase activity is likely to be minor.

We questioned how much thioesterase activity within mitochondria is attributable to each Acot. Here, we used a new mouse model of Acot2 loss to estimate the contribution of Acot2 to the total mitochondrial thioesterase activity. We generated mice with floxed Acot2 alleles ($Acot2^{fl/fl}$), from which germ line whole-body Acot2 knockout ($Acot2^{-/-}$) mice were generated (Fig. 3*B*). Mitochondria from these mice were used to estimate Acot2-specific activity. First, the possibility of compensatory up-regulation of other mitochondrial Acots was considered. $Acot2^{-/-}$ mice had higher mRNA for Acot9 in liver and Acot13 in kidney and skeletal muscle (Fig. 3*C*), but protein levels were unchanged (Fig. 3*D*). Acot15 mRNA was higher in all $Acot2^{-/-}$ tissues (Fig. 3*C*), but the protein is unlikely to be higher because thioesterase activity for its major substrate, C18:3-CoA, was unchanged (Fig. 3*E*).

Fig. 3*E* depicts thioesterase activity in five tissues from $Acot2^{-/-}$ mice. Acot2-specific activity was estimated as the difference in the average activity from mitochondria from control and $Acot2^{-/-}$ mice (Fig. 3*F*). Values for C4:0- and C8:0-CoA in the $Acot2^{-/-}$ samples were within the variability of the control samples (Fig. 3*A*). Thus, $Acot2^{-/-}$ samples only showed activity for C14:0-, C16:0-, and C16:1-CoA, and very low activity for C18:3-CoA, consistent with the expected substrate specificity for Acot2 (11). Acot2-specific thioesterase activity for these substrates in heart, skeletal muscle, kidney, and BAT was 2–5 nmol/min/mg. Liver mitochondria expressed very little Acot2-specific activity.

In the $Acot2^{-/-}$ samples, activity toward C16:0- and C16:1-CoA in heart, skeletal muscle, BAT, and kidney likely reflects activity of only Acot13 because Acot7 is minimally expressed in those tissues and Acot9 has minimal activity for those sub-

Figure 3. Tissue-specific mitochondrial thioesterase activity and contribution of Acot2. *A*, thioesterase activity in mitochondria from mouse tissues (*skm*, skeletal muscle) for a range of acyl-CoAs. Statistical analysis was by one-way ANOVA, Tukey post hoc tests. **, $p < 0.05$, liver *versus* all other organs; *, $p < 0.05$ *versus* heart and liver; #, $p < 0.05$, liver *versus* skeletal muscle, heart, and kidney; $, $p < 0.05$, skeletal muscle and liver *versus* BAT and kidney. Values are mean ± S.E. (*error bars*); $n = 6–8$. *B*, Acot2 whole-body knockout mouse ($Acot2^{-/-}$) model generated by crossing mice with floxed Acot2 alleles (*fl/fl*) with mice expressing Cre recombinase driven by the ella promoter. Knockout was validated by PCR and Western blotting (*wb*) analysis using isolated mitochondria. *Arrow*, faint Acot2 band in fl/fl liver mitochondria. *C* and *D*, evaluation of possible compensatory changes (mRNA (*C*) and mitochondrial protein (*D*)) in the expression of other mitochondrial Acots in $Acot2^{-/-}$ mice. The amount of protein loaded was 30 μg for Acot2 and Acot9, 40 μg for Acot7, and 5 μg for Acot13 and Complex I (*C - I*). Statistical analysis in *C* was by *t* test (levels in $Acot2^{-/-}$ *versus* floxed control mice): *, **, and ***, $p = 0.05$, $p = 0.03$, and $p = 0.01$, respectively. *E*, thioesterase activity in mitochondria from the indicated tissues harvested from $Acot2^{-/-}$ mice. Values are mean ± S.E.; $n = 4–5$. *F*, Acot2-specific thioesterase activity calculated by subtracting activity measured in $Acot2^{-/-}$ mitochondria (*E*) from activity measured in mitochondria from floxed mice (*A*). *Error bars* in *F*, Gaussian error propagation (calculated as the square root of the sum of the variances).

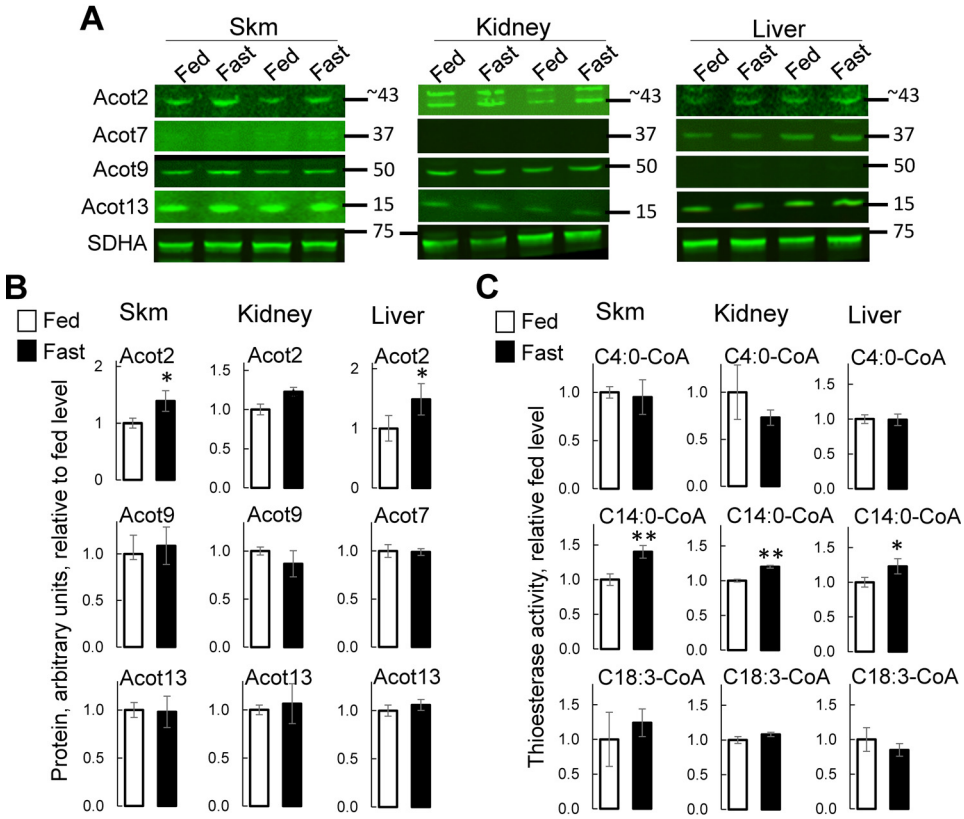

Figure 4. Fasting induces only small changes in mitochondrial Acot protein and thioesterase activity. Protein levels (*A* and *B*) and thioesterase activity (*C*) of Acots in mitochondria isolated from the indicated tissues harvested from overnight fasted mice (~9 a.m. tissue harvest) and *ad libitum* fed mice (~5 p.m. tissue harvest). Harvest times matched points of highest and lowest Acot2 mRNA expression (29). In *A* and *B*, values are mean ± S.E. (*error bars*); n = 4–5/condition. *, $p = 0.05$; **, $p = 0.02$, unpaired t test. In *A*, the amount of protein loaded was 30 μg for Acot2 and Acot9, 40 μg for Acot7, and 5 μg for Acot13 and SDHA.

strates. Acot13 activity can be estimated as 2–3 nmol/min/mg toward C16:1-CoA and ~1 nmol/min/mg toward C16:0-CoA except in BAT, where it is ~3 nmol/min/mg.

In summary, the highest thioesterase activity in mitochondria is toward C4:0-CoA, catalyzed by Acot9, and is 3–10 times higher than activity toward C14:0-, C16:0-, and C16:1-CoA, which are catalyzed to a similar extent by Acot2 and Acot13. Activity toward C18:1- and C18:3-CoA is very low, suggesting only a minor contribution of Acot15 to matrix thioesterase activity. Finally, BAT, kidney, heart, and, skeletal muscle mitochondria expressed far more thioesterase activity than liver mitochondria.

Regulation of matrix Acots

Some Acots are transcriptionally regulated by PPAR agonists, and nutritional stimuli such as high-fat feeding and fasting studies have mainly shown this at the mRNA level (3, 19, 21, 29, 31), but some also at the protein level (11, 21, 27, 32). Furthermore, Acot2 mRNA in the mouse heart oscillates with the time of day, with the lowest expression near the end of the light phase (29). Thus, mitochondrial Acot activity may be more prevalent at certain times of the day due to time-dependent effects on gene regulation. To test this, we measured Acot protein abundance and activity in mitochondria from liver, skeletal muscle, and kidney from overnight fasted mice and compared it with that from mice ~2 h before the end of the light phase. With fasting, Acot2 protein rose by ~20%, whereas protein levels of Acot9, Acot7, and Acot13 did not change (Fig. 4, *A* and *B*). Likewise, thioesterase activity in mitochondria from fasted mice was only increased for Acot2 substrates (Fig. 4*C*). Thus, although some Acots are readily induced by PPAR agonists and high-fat feeding, induction by physiological stimuli appears to be milder.

Beyond transcriptional regulation, there is some information on allosteric and other regulation of the Acots. However, this information is incomplete and does not include potential allosteric regulators of Acot2 or of Acot13 that would be relevant for its matrix localization. The activity of Acot1 (~98% identical to Acot2 at the amino acid level (1)) was reported to not be regulated by CoA, although data were not shown (33). Using liver mitochondria overexpressing Acot2 (23) and hydrolyzing C14:0-CoA, Acot2 activity was insensitive to CoA up to 200 μM (Fig. 5, *A* and *B*). Because Acot9 was strongly inhibited by NADH (IC_{50} of ~300 μM for C3:0-CoA and ~500 μM for C14:0-CoA) (5), we tested the sensitivity of Acot2 and -13 activity to NADH and NAD^+ and found that neither Acot2 nor Acot13 was substantially changed by 1 mM NADH or NAD^+ (Fig. 5, *A* and *B*). We also tested for sensitivity toward ADP and ATP and found that Acot2 and Acot13 activity was inhibited by ~20% by 10 mM ADP or ATP (Fig. 5, *A* and *B*).

CoA inhibits Acot7 and Acot9 (5, 34). For Acot9, the [CoA] at which activity was 50% inhibited (IC_{50}) was ~100 μM with C3:0-CoA and ~150 μM with C14:0-CoA. Although it is diffi-

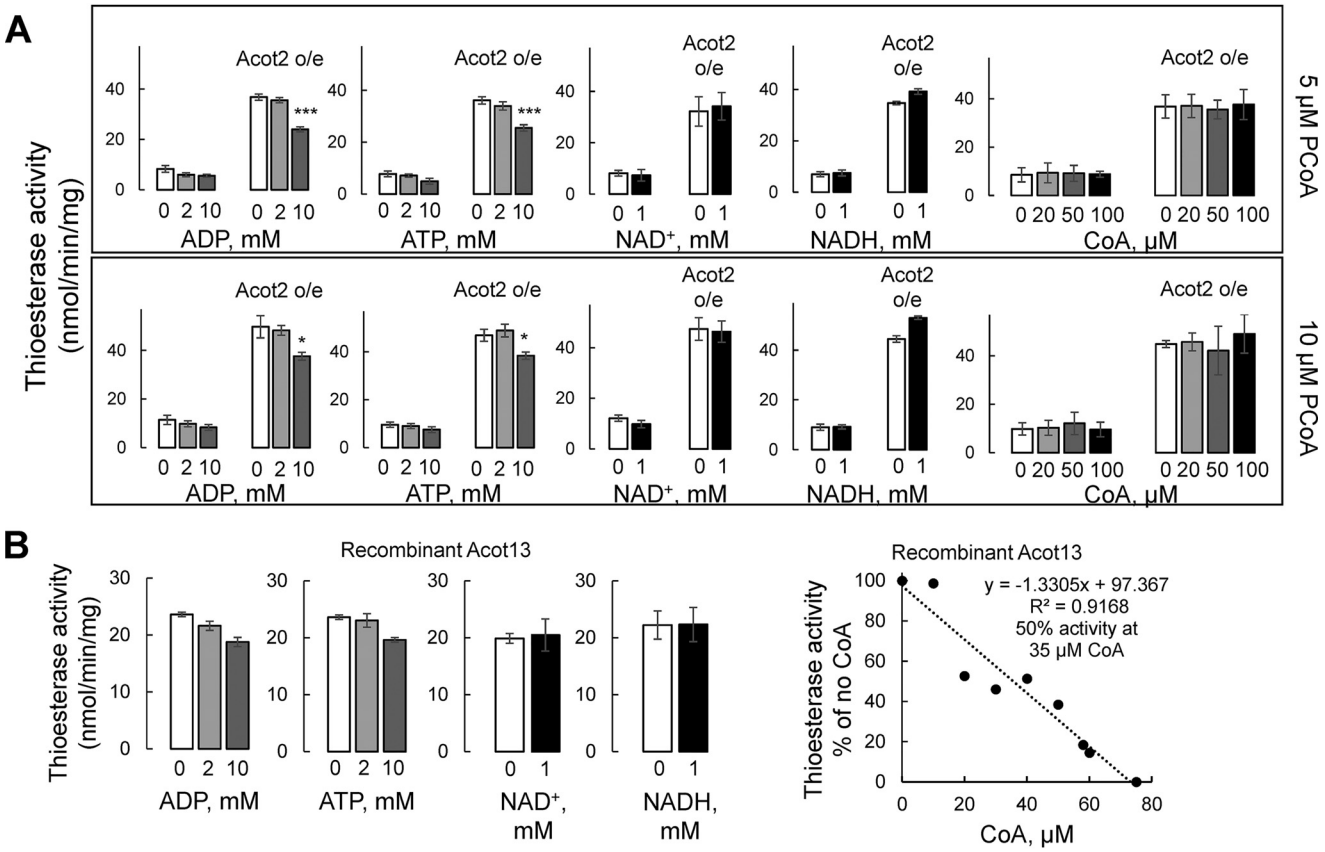

Figure 5. Distinct allosteric regulation of mitochondrial Acots. *A*, allosteric regulation of Acot2. Shown is Acot2-specific thioesterase activity toward 5 and 10 μM C16:0-CoA (palmitoyl-CoA: PCoA) in liver mitochondria without and with Acot2 overexpression. Values are mean ± S.E. (*error bars*); $n = 4–6$. *, $p = 0.02$; ***, $p < 0.001$; both p values are 10 mM *versus* 0 mM ADP or ATP and 10 mM *versus* 2 mM ADP or ATP; two-way ANOVA, Tukey post hoc tests. *B*, allosteric regulation of recombinant Acot13, using C14:0-CoA (10 μM) as the substrate. Values are mean ± S.E.; $n = 4$ technical replicates.

cult to accurately ascertain [CoA] within the matrix, inhibition of Acot activity by 100–150 μM CoA is likely to be physiologically relevant. To determine whether Acot13 is inhibited by CoA, we used recombinant mouse Acot13 (3); activity toward C14:0-CoA was strongly inhibited by CoA with an IC_{50} of ~35 μM (Fig. 5*B*).

StarD2 (also known as phosphatidylcholine transfer protein) interacts with Acot13 (35). Recombinant StarD2 approximately doubled the V_{max} of recombinant Acot13 (3, 35); thus, StarD2 could be considered as a regulator of Acot13. Because a significant fraction of Acot13 is in the matrix, we asked whether StarD2 was also present. Using the protease protection approach, StarD2 was associated with mitochondria (Fig. 6*A*), as reported (3), and also with the post-nuclear supernatant fraction of the 8000 × *g* spin, consistent with its presence also in the cytosol (3). Mitochondria-associated StarD2 was fully cleaved by trypsin alone, analogous to Tom20 (Fig. 6*A*). Trypsin also cleaved Tim23, and we had trouble obtaining conditions distinguishing Tim23 and Tom20. Thus, StarD2 localizes to the OMM, IMM, and/or intermembrane space. If it is in the matrix, its abundance is very low. Thus, the majority of matrix Acot13 would not be influenced by StarD2.

The interaction of StarD2 with Acot13 in the liver was shown to increase during the early phase of refeeding after mice were fasted overnight (8). Moreover, StarD2 localization to mitochondria increased with PPAR agonist treatment (36). Thus, we asked whether the fraction of Acot13 available to be regulated by StarD2 depends on nutrient availability. We questioned whether fasting and refeeding are associated with a redistribution of Acot13 away from mitochondria, whether Acot13 associates with the OMM during refeeding, and whether the association of StarD2 with mitochondria changes. Thus, we fractioned the liver from fed and overnight fasted mice, and from mice fasted and then refed for 2 or 5 h, and then performed protease protection experiments on the 8000 × *g* pellet. Fasting did not influence the amount of StarD2 associated with mitochondria (Fig. 6*B*). Comparing fasting with refeeding, the amount of StarD2 or Acot13 associated with mitochondria was similar (Fig. 6*C*), as was the localization of mitochondrial Acot13 to the matrix and StarD2 to the OMM/IMS/IMM (Fig. 6*D*).

Discussion

Here, we undertook a comparison of mitochondrial thioesterases, in terms of activity, expression level, and regulation, among mitochondria from different tissues to provide insight into why there are so many matrix-localized Acots. It was already suggested that several matrix Acots co-existed, some with an overlapping tissue expression and substrate specificity, raising the question of whether some matrix Acots are redundant. Alternatively, different matrix Acots could have unique roles, defined by tissue specificity and/or regulation. These are important questions, as matrix Acots are poised to regulate

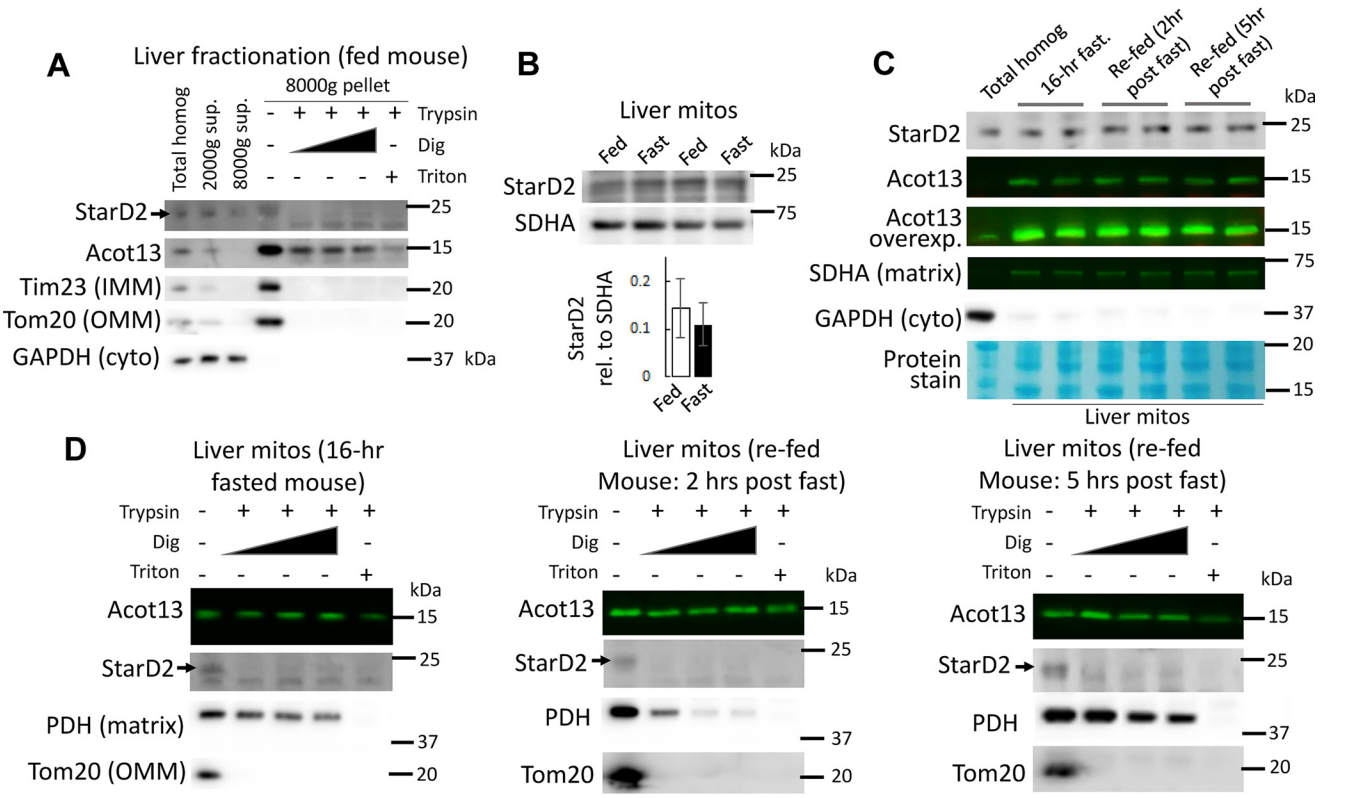

Figure 6. Co-localization of Acot13 and its regulator StarD2 is minimal for the matrix Acot13 pool, even after major nutrient perturbations. *A*, liver fractionation and protease protection experiment on the 8000 × *g* pellet fraction of liver from a fed mouse. GADPH was used as a cytoplasmic (*cyto*) marker. *Sup.*, supernatant. *B*, mitochondrial fraction from liver harvested from *ad libitum* fed or overnight fasted mice. *Bar chart*, mean ± S.E. (*error bars*), $n = 5$/condition; no significant difference (unpaired *t* test). *C*, mitochondrial (8000 × *g* pellet) fraction from liver harvested from mice fasted overnight or fasted overnight and then refed for 2 or 5 h; *D*, protease protection experiments from these mitochondria. *A* and *D*, further details about protease protection experiments are available in the legend to Fig. 1. In all *panels*, 10 μg of protein were loaded.

mitochondrial β-oxidation, which is susceptible to overload with consequences for β-oxidation itself (6, 37), for other matrix pathways, and ultimately for other aspects of cell function. Thus, understanding the characteristics of Acots, both individually and as a group, should provide insight into how Acots influence β-oxidation and how best to study the matrix Acots. The current study sought to fill key gaps and provide easy comparisons among thioesterase activities and expression of Acots in mitochondria from several mouse tissues.

The main findings are summarized in Fig. 7. Our study is the first to establish that Acot7, Acot9, and Acot13 localize to the matrix. This finding is important in light of the existing data on the biological role of Acot13 (2, 8). Second, all mitochondria surveyed, except from liver, robustly expressed Acot2, Acot9, and Acot13. Liver, in contrast, expressed some Acot7 and Acot13 and low levels of Acot2. This pattern of mitochondrial Acot expression and activity across tissues highlights the potential importance of Acots in tissues such as kidney, skeletal muscle, and heart, where Acots are understudied. Third, Acot9 protein was previously shown to be very low in skeletal muscle, with a band shifted higher in molecular weight, and to be undetectable in heart (5). Here we show substantial thioesterase activity for C4:0-CoA in heart and skeletal muscle mitochondria. Acot9 is the only matrix Acot that hydrolyzes C4:0-CoA, and skeletal muscle and heart expressed Acot9 at a molecular weight similar to that in BAT and kidney (5) (this work). Thus, Acot9 is expressed in heart and even more so in glycolytic skeletal muscle. Fourth, the most important source of regulation of the Acots, specifically Type II Acots, was from CoA. In contrast, Acot2, a Type I Acot, was not regulated by CoA; nor was it substantially regulated by the potential allosteric regulators we tested, raising the possibility that Acot2 is constitutively active, but at a low level based on the estimate obtained from Acot2$^{-/-}$ mitochondria. Altogether, these observations reveal that, despite potential redundancy due to some overlap in tissue expression and substrate specificity, different matrix Acots may occupy different functional roles determined mainly by regulation (Acot7, -9, and -13 *versus* Acot2) and substrate specificity (Acot9 *versus* Acot2 and -13).

Our study also highlights that, in contrast to the robust upregulation of Acot mRNA by pharmacologic induction of PPARs (3, 19, 21, 29, 31), fasting, a physiological stimulus of PPARs, had a minimal impact on mitochondrial Acot expression or activity. Thus, despite pharmacological approaches suggesting PPAR induction of Acot mRNA as an important means of regulating Acots, regulation by CoA of Type II Acots may be quantitatively the most important physiological means of regulating the activity of matrix Acots (Type II only).

Finally, because StarD2 can increase Acot13 activity (3), we determined whether StarD2 could regulate matrix-localized Acot13. However, our findings suggest that matrix-localized Acot13 would be minimally or not influenced by StarD2 under a number of physiological conditions. These results are noteworthy because the amount of Acot13 that associates with

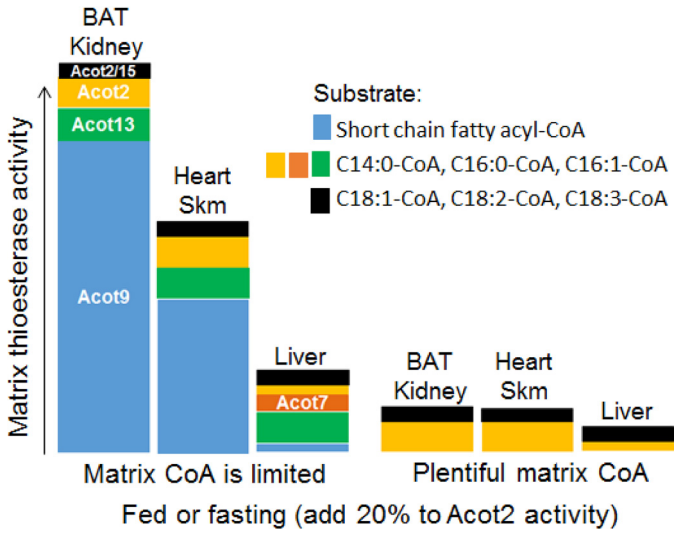

Figure 7. Summary of findings. Mitochondrial matrix Acots reside in different functional niches based on substrate specificity, sensitivity to CoA inhibition, and tissue-specific expression. We have localized Acot7, -9, and -13 to the mitochondrial matrix (Fig. 1), joining Acot2 and -15 that were previously localized to the matrix. The *total height* of the *columns* represents the approximate thioesterase activity for all substrates tested, based on data from Fig. 3. *Different colors* represent thioesterase activity for a particular substrate or group of substrates, as indicated by the legend. The *height* of each *differently colored column* (*i.e.* activity toward a particular substrate) represents the fractional contribution of that substrate to the total thioesterase activity in mitochondria from the indicated tissue. *Acot inside* the *columns*, the Acot family member that would be responsible for the thioesterase activity represented by the *color* of the *column* (based on data from Fig. 2). For each tissue, columns are shown for CoA-limiting (*left grouping* of *columns*) and CoA-replete conditions (*right grouping* of *columns*). BAT and kidney mitochondria show the highest total potential thioesterase activity, contributed primarily by activity toward short-chain fatty acyl-CoAs, whereas liver mitochondria would have very low thioesterase activity, even under CoA-limited conditions. CoA was by far the strongest regulator of Acot9 and -13, and Acot2 was minimally regulated by multiple potential allosteric regulators (see Fig. 5); a CoA-limited condition would increase thioesterase activity for Acot7, -9, and -13 substrates, but not for Acot2 substrates. Thus, we propose a model in which Acot2 provides a constitutive overflow pathway for acyl-CoAs that are likely primarily destined for β-oxidation, whereas Acot7, -9, and -13 would provide an overflow pathway that depends on the local CoA concentration. Physiological activation of PPAR activity by fasting had only a small effect on Acot2 activity (and protein level) (based on data from Fig. 4), despite the substantial inducibility of Acot2 by PPAR agonists reported in the literature. *Skm*, skeletal muscle.

StarD2 was higher in the liver of mice that were refed after an overnight fast (8). Our findings suggest that this greater association of Acot13 and StarD2 involved the cytoplasmic pools of these proteins, whereas the matrix pool of Acot13 was unperturbed. More generally, our data indicate that there are two pools of Acot13, namely a cytoplasmic pool that can interact variably with StarD2 and a matrix pool that is largely sequestered from StarD2.

Acot13 localizes to the mitochondrial matrix

Using two different proteases and mitochondria from three different tissues, we provide evidence that Acot13 localizes to the mitochondrial matrix, even though the prediction of an N-terminal MTS or an internal targeting sequence is low (~30%).

Two studies document that the acetylated proteome of mouse liver mitochondria showed a significant acetylation of residue Lys-13 of Acot13 that depended on the matrix deacetylase Sirt3 (38, 39). Sirt3-dependent acetylation of Acot13 was also observed in heart mitochondria, although the specific residue was not indicated (40). Further analysis of these acetylated proteomes revealed that established OMM proteins with acetylated lysines did not have any that were Sirt3-dependent. These observations further support the matrix localization of Acot13.

Regulation of matrix Acots

We found Acot13 to be strongly inhibited by CoA (Fig. 5), as reported for Acot7 and Acot9 (5, 34). Although it is difficult to measure [CoA] in the matrix, the [CoA] that inhibits Acot9 (IC_{50} = 100 μM) and Acot13 (IC_{50} ~35 μM) is expected to fall within the physiological range of [CoA], positioning these Acots as safety valves gated by CoA. Heart, skeletal muscle, kidney, and BAT mitochondria substantially expressed Acot9 and Acot13 (Fig. 3), which, together, have a substrate specificity covering short- to long-chain acyl-CoAs. Thus, the ability to expand the capacity of thioesterase activity in response to low [CoA] would apply across a wide range of fatty acyl-CoAs in these tissues. In contrast, liver mitochondria expressed little Acot9. Thus, CoA gating would only occur in liver mitochondria for long-chain acyl-CoAs, via Acot13.

Acot2 activity was only slightly inhibited by ADP and ATP and was unaffected by the other potential allosteric regulators we tested, including CoA. It is possible that acetylation regulates Acot2 activity because two acetylated lysine residues appeared in mitochondrial protein acetylation screens (38, 39). Based on the crystal structure of human Acot2 (41), one of these lysines (Lys-345 in human Acot2) is near the active site but pointed away from it. The other lysine (Lys-104 in human Acot2) is in a loop that could serve as a flap over the active site; because acetylation imparts a negative charge, and CoA is negatively charged, Lys-104 acetylation might alter substrate binding. However, the acetylation state of both lysine residues was insensitive to Sirt3 (38, 39).

Considerations for evaluating the role of matrix Acots in β-oxidation

For all matrix Acots, the obvious competing pathway is β-oxidation because the fatty acyl-CoA dehydrogenases could compete directly for fatty acyl-CoA substrates. Competition would be on the basis of substrate specificity and K_m; K_m values for Acot2 and -13 are similar to those of the long-chain acyl-CoA dehydrogenases (42). Because short-chain methyl-branched acyl-CoAs are also substrates for Acot9, a role in amino acid oxidation was also proposed (5) but has not yet been tested.

To determine the potential impact of matrix thioesterase activity on β-oxidation, values of thioesterase activity (Fig. 3) can be compared with β-oxidation rates. The heart is a useful test case because there are substantial data on palmitate oxidation using [9,10-^{3}H]palmitate, which directly assesses acyl-CoA dehydrogenase flux. In working heart preparations, the palmitate oxidation rate is ~15 nmol/min/mg of mitochondrial protein (based on ~1200 nmol/min/dry heart weight and mitochondria at 2% of wet heart weight) (43–45). In heart mitochondria, maximal thioesterase activity toward C16:0-CoA was not much less, at ~6 nmol/min/mg. If activity for C14:0-CoA, C4:0-, and C8-CoA is taken into account, and considering that β-oxidation rates are lower in other

tissues, thioesterase activity could theoretically outstrip palmitate oxidation.

Direct evidence that a β-oxidation substrate can be hydrolyzed to fatty acid and, thus, that β-oxidation can compete with thioesterase activity, was shown by supplying mitochondria with [^{14}C]palmitoylcarnitine (20 μM) and then measuring [^{14}C]palmitate production by TLC (20, 24). Palmitate was produced at ~0.03 nmol/min/mg mitochondrial protein in skeletal muscle mitochondria (24) and 0.5 nmol/min/mg mitochondrial protein in heart mitochondria (20). These values are 1–2 orders of magnitude lower than the maximal thioesterase activity for palmitoyl-CoA, suggesting that matrix thioesterases offer far less competition for β-oxidation than is predicted by maximal thioesterase activity and K_m values alone. Possible explanations for this discrepancy include unknown regulators of the Acots and an *in vivo* limitation on substrate accessibility to the Acots, either due to tight substrate channeling within β-oxidation (46) or because the Acots are located apart from the β-oxidation enzymes. Also, CoA inhibition of Acot9 and Acot13 could remove much of the Acot competition on palmitate oxidation when CoA is abundant.

Possible unique functional roles for matrix Acots in the context of β-oxidation

Evidence that Type II matrix Acots have a unique functional role that depends on CoA abundance supports the idea these Acots mitigate CoA limitation, as originally proposed by Himms-Hagen and Harper (47). However, the CoA independence of Acot2 activity implies an additional role for matrix Acots. This role might be as a minimally regulated siphon that removes long-chain fatty acyl-CoA from β-oxidation.

An ability of matrix Acots to compete with β-oxidation implies that matrix processes can exert control over β-oxidation, a concept that conflicts with the generally accepted model that the main control point for β-oxidation is the entry of activated long-chain fatty acids into mitochondria by CPT1 (carnitine palmitoyltransferase-1) at the OMM. However, recent experimental and modeling studies show that control of β-oxidation can be partly or substantially taken over by the β-oxidation reactions themselves (6, 37). The possibility that β-oxidation enzymes exert control over β-oxidation was also suggested by measurements of β-oxidation intermediates (48). More recent modeling studies indicate that, at high C16:0-CoA concentration, control of β-oxidation shifts to the C4-C6 reactions of medium-chain ketoacyl-CoA thiolase (MCKAT) (6). This potential for overload, which could theoretically deplete CoA and halt β-oxidation (6), suggests the utility of the Acots to mitigate gridlock at MCKAT and to prevent CoA depletion. This model of β-oxidation does not include Acot reactions (6, 37). The present study facilitates the incorporation of the Acots.

Conclusions

We have determined that Acot7, Acot9, and Acot13 reside in the mitochondrial matrix, joining Acot2 and Acot15. Furthermore, we report that these matrix Acots are specialized according to substrate specificity and sensitivity to CoA inhibition (Type II Acots). Thus, the functional relevance of Type II matrix Acots should increase with decreasing [CoA] to ensure that CoA does not become limiting (*i.e.* for β-oxidation or branched-chain amino acid catabolism). However, our study also reveals that Acot2 is minimally influenced by factors within the matrix, including CoA. Thus, Acot2 may be a constitutively active matrix thioesterase and have a role beyond mitigating CoA limitation.

Materials and methods

Details are provided in the supporting information.

Reagents

Acyl-CoA esters were purchased from Avanti Polar Lipids and used for no longer than 2 months after dilution. Most other reagents were purchased from Sigma–Aldrich with the exception of antibodies and recombinant Acot13.

Control and Acot2 knockout mice

10–14-Week-old male were used in accordance with protocol 01307 approved by the Thomas Jefferson University Institutional Animal Care and Use Committee. C57BL/6J mice or whole-body Acot2 knockout mice (Acot2$^{-/-}$) were generated from our breeding colony. The strategy used to generate mice with floxed Acot2 alleles (Acot2$^{fl/fl}$) and Acot2$^{-/-}$ mice is described in the legend to Fig. 3*B* and the supporting information. Mice were maintained on a 12-h/12-h light/dark cycle (lights on: 7 a.m. to 7 p.m.) and *ad libitum* fed a standard diet (LabDiet 5001, Purina). Some mice were fasted overnight (7 p.m. to 9 a.m.). Mitochondria from whole-body Acot13 knockout mice (8) were isolated in the laboratory of Dr. David Cohen.

Expression of recombinant Acot2 in mouse liver

Adenovirus harboring mouse Acot2 cDNA or empty vector control (2×10^9 pfu/mouse; as in Ref. 23) was diluted in saline and then administered to mice via the tail vein, as in Ref. 23. Liver mitochondria were isolated 7 days after injection. Localization of Acot2 to mitochondria and not to cytosol was previously confirmed, as well as the appropriate substrate specificity for Acot2 (23).

Recombinant Acot13 protein

Mouse recombinant Acot13 (generous gift from David Cohen, Weill Cornell Medical College) was generated as described (3). Briefly, Acot13 with an N-terminal His_{10} tag was generated in *Escherichia coli* BL21 (De3) cells, eluted in imidazole, dialyzed against 20 mM sodium-phosphate buffer (pH 7.4), and then run on an SDS-polyacrylamide gel, yielding a single band (see also Fig. 1*A*). The His_{10} tag was not removed.

Isolation of mitochondria from mouse tissues

Mice were sacrificed by cervical dislocation at ~9 a.m. All media were ice-cold, and the procedure was done on ice or at 4 °C. Protein of the final resuspended pellets was determined by bicinchoninic assay (BCA; Life Technologies, Inc.). Detailed protocols are provided in the supporting information.

Thioesterase activity

Thioesterase activity was measured in isolated mitochondria (23) or recombinant Acot13 protein (3), essentially as described (23).

Quantitative PCR and immunoblotting

Detailed procedures as well as information about primers and commercial antibodies is provided in the supporting information. Custom antibodies were used to recognize Acot2, Acot7, Acot9, Acot13, and StarD2 (generous gifts from, respectively, Stefan Alexson (Karolinska Institute), Michael Wolfgang (Johns Hopkins University), Stefan Alexson, and David Cohen (Weill Cornell Medical College) for Acot13 and StarD2). All are rabbit polyclonal antibodies. The anti-Acot2 antibody was generated using Acot2 purified from rat liver as the antigen (27). The anti-Acot7 antibody was generated using the peptide EKKRFEEGKGRYLQMK (corresponding to amino acids 355–370 of mouse Acot7 protein) as the antigen (26). The anti-Acot9 antibody was generated using the peptide CEEEELFKQGELNKS (corresponding to amino acids 225–238 of mouse ACOT9 protein Acot9) as the antigen (5). The anti-Acot13 antibody was generated using the peptide EKVTLVSAAPEKLIC (corresponding to amino acids 26–40 of mouse Acot13 protein) as the antigen (3). The anti-StarD2 antibody was generated against the last 15 amino acids at the C terminus of human StarD2 (49). Note that amino acids are given with reference to the protein containing the mitochondrial targeting sequence.

Protease protection experiments

Reactions were run for 15 min, at room temperature, in a total volume of 40 μl of MAS, using 2.5 mg/ml mitochondria. During the assay, we tested different concentrations of trypsin (0.068, 0.102, 0.152, and 0.204 mg/ml final concentration for each reaction) as well as proteinase K (0.01 or 0.02 mg/ml final concentration). Digitonin was added at a final concentration of 1, 1.25, or 1.5 μg/μl, and Triton was added at a final concentration of 1 or 2%. Reactions were stopped by 10-min incubation at room temperature with 3.25 mM phenylmethylsulfonyl fluoride.

Statistical analysis

Bar charts show the mean and S.E. Statistical analysis was done using either a Student's *t* test or analysis of variance followed by Tukey post hoc tests, as appropriate; details are provided in the figures and figure legends. SigmaPlot was used to perform the statistical analysis. Further details of the statistical analysis are described throughout.

Author contributions—C. B., F. B., J. M. H., and E. L. S. conceptualization; C. B., L. A.-P., K. B., F. B., Y. S., and E. L. S. formal analysis; C. B., L. A.-P., K. B., F. B., Y. S., and E. L. S. investigation; C. B., F. B., and E. L. S. methodology; C. B. and E. L. S. writing-original draft; C. B., F. B., J. M. H., and E. L. S. writing-review and editing; C. B., F. B., and E. L. S. data curation; J. M. H. and E. L. S. supervision; E. L. S. funding acquisition; E. L. S. validation; E. L. S. project administration.

Acknowledgments—We thank Megan Roche and Cynthia Moffat for contributions to preliminary experiments.

References

1. Hunt, M. C., Rautanen, A., Westin, M. A., Svensson, L. T., and Alexson, S. E. (2006) Analysis of the mouse and human acyl-CoA thioesterase (ACOT) gene clusters shows that convergent, functional evolution results in a reduced number of human peroxisomal ACOTs. *FASEB J.* **20,** 1855–1864 CrossRef Medline
2. Tillander, V., Alexson, S. E. H., and Cohen, D. E. (2017) Deactivating fatty acids: acyl-CoA thioesterase-mediated control of lipid metabolism. *Trends Endocrinol. Metab.* **28,** 473–484 CrossRef Medline
3. Wei, J., Kang, H. W., and Cohen, D. E. (2009) Thioesterase superfamily member 2 (Them2)/acyl-CoA thioesterase 13 (Acot13): a homotetrameric hotdog fold thioesterase with selectivity for long-chain fatty acyl-CoAs. *Biochem. J.* **421,** 311–322 CrossRef Medline
4. Hunt, M. C., Solaas, K., Kase, B. F., and Alexson, S. E. (2002) Characterization of an acyl-coA thioesterase that functions as a major regulator of peroxisomal lipid metabolism. *J. Biol. Chem.* **277,** 1128–1138 CrossRef Medline
5. Tillander, V., Arvidsson Nordström, E., Reilly, J., Strozyk, M., Van Veldhoven, P. P., Hunt, M. C., and Alexson, S. E. (2014) Acyl-CoA thioesterase 9 (ACOT9) in mouse may provide a novel link between fatty acid and amino acid metabolism in mitochondria. *Cell Mol. Life Sci.* **71,** 933–948 CrossRef Medline
6. Martines, A. M. F., van Eunen, K., Reijngoud, D. J., and Bakker, B. M. (2017) The promiscuous enzyme medium-chain 3-keto-acyl-CoA thiolase triggers a vicious cycle in fatty-acid β-oxidation. *PLoS Comput. Biol.* **13,** e1005461 CrossRef Medline
7. Franklin, M. P., Sathyanarayan, A., and Mashek, D. G. (2017) Acyl-CoA thioesterase 1 (ACOT1) regulates PPARα to couple fatty acid flux with oxidative capacity during fasting. *Diabetes* **66,** 2112–2123 CrossRef Medline
8. Ersoy, B. A., Maner-Smith, K. M., Li, Y., Alpertunga, I., and Cohen, D. E. (2018) Thioesterase-mediated control of cellular calcium homeostasis enables hepatic ER stress. *J. Clin. Invest.* **128,** 141–156 CrossRef Medline
9. Kang, H. W., Niepel, M. W., Han, S., Kawano, Y., and Cohen, D. E. (2012) Thioesterase superfamily member 2/acyl-CoA thioesterase 13 (Them2/Acot13) regulates hepatic lipid and glucose metabolism. *FASEB J.* **26,** 2209–2221 CrossRef Medline
10. Tillander, V., Miniami, A., Alves-Bezerra, M., Coleman, R. A., and Cohen, D. E. (2019) Thioesterase superfamily member 2 promotes hepatic insulin resistance in the setting of glycerol-3-phosphate acyltransferase 1-induced steatosis. *J. Biol. Chem.* **294,** 2009–2020 CrossRef Medline
11. Svensson, L. T., Engberg, S. T., Aoyama, T., Usuda, N., Alexson, S. E., and Hashimoto, T. (1998) Molecular cloning and characterization of a mitochondrial peroxisome proliferator-induced acyl-CoA thioesterase from rat liver. *Biochem. J.* **329**, 601–608 CrossRef Medline
12. Zhuravleva, E., Gut, H., Hynx, D., Marcellin, D., Bleck, C. K., Genoud, C., Cron, P., Keusch, J. J., Dummler, B., Esposti, M. D., and Hemmings, B. A. (2012) Acyl coenzyme A thioesterase Them5/Acot15 is involved in cardiolipin remodeling and fatty liver development. *Mol. Cell. Biol.* **32,** 2685–2697 CrossRef Medline
13. Chen, D., Latham, J., Zhao, H., Bisoffi, M., Farelli, J., and Dunaway-Mariano, D. (2012) Human brown fat inducible thioesterase variant 2 cellular localization and catalytic function. *Biochemistry* **51,** 6990–6999 CrossRef Medline
14. Backes, S., Hess, S., Boos, F., Woellhaf, M. W., Gödel, S., Jung, M., Mühlhaus, T., and Herrmann, J. M. (2018) Tom70 enhances mitochondrial preprotein import efficiency by binding to internal targeting sequences. *J. Cell Biol.* **217,** 1369–1382 CrossRef Medline
15. Morgenstern, M., Stiller, S. B., Lübbert, P., Peikert, C. D., Dannenmaier, S., Drepper, F., Weill, U., Höss, P., Feuerstein, R., Gebert, M., Bohnert, M., van der Laan, M., Schuldiner, M., Schütze, C., Oeljeklaus, S., *et al.* (2017) Definition of a high-confidence mitochondrial proteome at quantitative scale. *Cell Rep.* **19,** 2836–2852 CrossRef Medline
16. Calvo, S. E., Clauser, K. R., and Mootha, V. K. (2016) MitoCarta2.0: an updated inventory of mammalian mitochondrial proteins. *Nucleic Acids Res.* **44,** D1251–D1257 CrossRef Medline
17. Ellis, J. M., Bowman, C. E., and Wolfgang, M. J. (2015) Metabolic and tissue-specific regulation of acyl-CoA metabolism. *PLoS One* **10,** e0116587 CrossRef Medline
18. Han, S., and Cohen, D. E. (2012) Functional characterization of thioesterase superfamily member 1/acyl-CoA thioesterase 11: implications for metabolic regulation. *J. Lipid Res.* **53,** 2620–2631 CrossRef Medline

19. Lanni, A., Mancini, F. P., Sabatino, L., Silvestri, E., Franco, R., De Rosa, G., Goglia, F., and Colantuoni, V. (2002) *De novo* expression of uncoupling protein 3 is associated to enhanced mitochondrial thioesterase-1 expression and fatty acid metabolism in liver of fenofibrate-treated rats. *FEBS Lett.* **525,** 7–12 CrossRef Medline
20. Gerber, L. K., Aronow, B. J., and Matlib, M. A. (2006) Activation of a novel long-chain free fatty acid generation and export system in mitochondria of diabetic rat hearts. *Am. J. Physiol. Cell Physiol.* **291,** C1198–C1207 CrossRef Medline
21. King, K. L., Young, M. E., Kerner, J., Huang, H., O'Shea, K. M., Alexson, S. E., Hoppel, C. L., and Stanley, W. C. (2007) Diabetes or peroxisome proliferator-activated receptor α agonist increases mitochondrial thioesterase I activity in heart. *J. Lipid Res.* **48,** 1511–1517 CrossRef Medline
22. Fujita, M., Momose, A., Ohtomo, T., Nishinosono, A., Tanonaka, K., Toyoda, H., Morikawa, M., and Yamada, J. (2011) Upregulation of fatty acyl-CoA thioesterases in the heart and skeletal muscle of rats fed a high-fat diet. *Biol. Pharm. Bull.* **34,** 87–91 CrossRef Medline
23. Moffat, C., Bhatia, L., Nguyen, T., Lynch, P., Wang, M., Wang, D., Ilkayeva, O. R., Han, X., Hirschey, M. D., Claypool, S. M., and Seifert, E. L. (2014) Acyl-CoA thioesterase-2 facilitates mitochondrial fatty acid oxidation in the liver. *J. Lipid Res.* **55,** 2458–2470 CrossRef Medline
24. Seifert, E. L., Bézaire, V., Estey, C., and Harper, M. E. (2008) Essential role for uncoupling protein-3 in mitochondrial adaptation to fasting but not in fatty acid oxidation or fatty acid anion export. *J. Biol. Chem.* **283,** 25124–25131 CrossRef Medline
25. Momose, A., Fujita, M., Ohtomo, T., Umemoto, N., Tanonaka, K., Toyoda, H., Morikawa, M., and Yamada, J. (2011) Regulated expression of acyl-CoA thioesterases in the differentiation of cultured rat brown adipocytes. *Biochem. Biophys. Res. Commun.* **404,** 74–78 CrossRef Medline
26. Ellis, J. M., Wong, G. W., and Wolfgang, M. J. (2013) Acyl coenzyme A thioesterase 7 regulates neuronal fatty acid metabolism to prevent neurotoxicity. *Mol. Cell. Biol.* **33,** 1869–1882 CrossRef Medline
27. Svensson, L. T., Alexson, S. E., and Hiltunen, J. K. (1995) Very long chain and long chain acyl-CoA thioesterases in rat liver mitochondria: identification, purification, characterization, and induction by peroxisome proliferators. *J. Biol. Chem.* **270,** 12177–12183 CrossRef Medline
28. Hunt, M. C., Nousiainen, S. E., Huttunen, M. K., Orii, K. E., Svensson, L. T., and Alexson, S. E. (1999) Peroxisome proliferator-induced long chain acyl-CoA thioesterases comprise a highly conserved novel multi-gene family involved in lipid metabolism. *J. Biol. Chem.* **274,** 34317–34326 CrossRef Medline
29. Stavinoha, M. A., RaySpellicy, J. W., Essop, M. F., Graveleau, C., Abel, E. D., Hart-Sailors, M. L., Mersmann, H. J., Bray, M. S., and Young, M. E. (2004) Evidence for mitochondrial thioesterase 1 as a peroxisome proliferator-activated receptor-α-regulated gene in cardiac and skeletal muscle. *Am. J. Physiol. Endocrinol. Metab.* **287,** E888–E895 CrossRef Medline
30. Yamada, J., Kurata, A., Hirata, M., Taniguchi, T., Takama, H., Furihata, T., Shiratori, K., Iida, N., Takagi-Sakuma, M., Watanabe, T., Kurosaki, K., Endo, T., and Suga, T. (1999) Purification, molecular cloning, and genomic organization of human brain long-chain acyl-CoA hydrolase. *J. Biochem.* **126,** 1013–1019 CrossRef Medline
31. Hunt, M. C., Lindquist, P. J., Peters, J. M., Gonzalez, F. J., Diczfalusy, U., and Alexson, S. E. (2000) Involvement of the peroxisome proliferator-activated receptor alpha in regulating long-chain acyl-CoA thioesterases. *J. Lipid Res.* **41,** 814–823 Medline
32. Moreno, M., Lombardi, A., De Lange, P., Silvestri, E., Ragni, M., Lanni, A., and Goglia, F. (2003) Fasting, lipid metabolism, and triiodothyronine in rat gastrocnemius muscle: interrelated roles of uncoupling protein 3, mitochondrial thioesterase, and coenzyme Q. *FASEB J.* **17,** 1112–1114 CrossRef Medline
33. Huhtinen, K., O'Byrne, J., Lindquist, P. J., Contreras, J. A., and Alexson, S. E. (2002) The peroxisome proliferator-induced cytosolic type I acyl-CoA thioesterase (CTE-I) is a serine-histidine-aspartic acid α/β hydrolase. *J. Biol. Chem.* **277,** 3424–3432 CrossRef Medline
34. Forwood, J. K., Thakur, A. S., Guncar, G., Marfori, M., Mouradov, D., Meng, W., Robinson, J., Huber, T., Kellie, S., Martin, J. L., Hume, D. A., and Kobe, B. (2007) Structural basis for recruitment of tandem hotdog domains in acyl-CoA thioesterase 7 and its role in inflammation. *Proc. Natl. Acad. Sci. U.S.A.* **104,** 10382–10387 CrossRef Medline
35. Kanno, K., Wu, M. K., Agate, D. S., Fanelli, B. J., Wagle, N., Scapa, E. F., Ukomadu, C., and Cohen, D. E. (2007) Interacting proteins dictate function of the minimal START domain phosphatidylcholine transfer protein/StarD2. *J. Biol. Chem.* **282,** 30728–30736 CrossRef Medline
36. de Brouwer, A. P., Westerman, J., Kleinnijenhuis, A., Bevers, L. E., Roelofsen, B., and Wirtz, K. W. (2002) Clofibrate-induced relocation of phosphatidylcholine transfer protein to mitochondria in endothelial cells. *Exp. Cell Res.* **274,** 100–111 CrossRef Medline
37. van Eunen, K., Simons, S. M., Gerding, A., Bleeker, A., den Besten, G., Touw, C. M., Houten, S. M., Groen, B. K., Krab, K., Reijngoud, D. J., and Bakker, B. M. (2013) Biochemical competition makes fatty-acid β-oxidation vulnerable to substrate overload. *PLoS Comput. Biol.* **9,** e1003186 CrossRef Medline
38. Hebert, A. S., Dittenhafer-Reed, K. E., Yu, W., Bailey, D. J., Selen, E. S., Boersma, M. D., Carson, J. J., Tonelli, M., Balloon, A. J., Higbee, A. J., Westphall, M. S., Pagliarini, D. J., Prolla, T. A., Assadi-Porter, F., Roy, S., Denu, J. M., and Coon, J. J. (2013) Calorie restriction and SIRT3 trigger global reprogramming of the mitochondrial protein acetylome. *Mol. Cell* **49,** 186–199 CrossRef Medline
39. Rardin, M. J., Newman, J. C., Held, J. M., Cusack, M. P., Sorensen, D. J., Li, B., Schilling, B., Mooney, S. D., Kahn, C. R., Verdin, E., and Gibson, B. W. (2013) Label-free quantitative proteomics of the lysine acetylome in mitochondria identifies substrates of SIRT3 in metabolic pathways. *Proc. Natl. Acad. Sci. U.S.A.* **110,** 6601–6606 CrossRef Medline
40. Nguyen, T. T., Wong, R., Menazza, S., Sun, J., Chen, Y., Wang, G., Gucek, M., Steenbergen, C., Sack, M. N., and Murphy, E. (2013) Cyclophilin D modulates mitochondrial acetylome. *Circ. Res.* **113,** 1308–1319 CrossRef Medline
41. Mandel, C. R., Tweel, B., and Tong, L. (2009) Crystal structure of human mitochondrial acyl-CoA thioesterase (ACOT2). *Biochem. Biophys. Res. Commun.* **385,** 630–633 CrossRef Medline
42. Ikeda, Y., Okamura-Ikeda, K., and Tanaka, K. (1985) Purification and characterization of short-chain, medium-chain, and long-chain acyl-CoA dehydrogenases from rat liver mitochondria: isolation of the holo- and apoenzymes and conversion of the apoenzyme to the holoenzyme. *J. Biol. Chem.* **260,** 1311–1325 Medline
43. Fillmore, N., Levasseur, J. L., Fukushima, A., Wagg, C. S., Wang, W., Dyck, J. R. B., and Lopaschuk, G. D. (2018) Uncoupling of glycolysis from glucose oxidation accompanies the development of heart failure with preserved ejection fraction. *Mol. Med.* **24,** 3 CrossRef Medline
44. Sung, M. M., Zordoky, B. N., Bujak, A. L., Lally, J. S., Fung, D., Young, M. E., Horman, S., Miller, E. J., Light, P. E., Kemp, B. E., Steinberg, G. R., and Dyck, J. R. (2015) AMPK deficiency in cardiac muscle results in dilated cardiomyopathy in the absence of changes in energy metabolism. *Cardiovasc. Res.* **107,** 235–245 CrossRef Medline
45. Kienesberger, P. C., Pulinilkunnil, T., Sung, M. M., Nagendran, J., Haemmerle, G., Kershaw, E. E., Young, M. E., Light, P. E., Oudit, G. Y., Zechner, R., and Dyck, J. R. (2012) Myocardial ATGL overexpression decreases the reliance on fatty acid oxidation and protects against pressure overload-induced cardiac dysfunction. *Mol. Cell. Biol.* **32,** 740–750 CrossRef Medline
46. Wang, Y., Mohsen, A. W., Mihalik, S. J., Goetzman, E. S., and Vockley, J. (2010) Evidence for physical association of mitochondrial fatty acid oxidation and oxidative phosphorylation complexes. *J. Biol. Chem.* **285,** 29834–29841 CrossRef Medline
47. Himms-Hagen, J., and Harper, M. E. (2001) Physiological role of UCP3 may be export of fatty acids from mitochondria when fatty acid oxidation predominates: an hypothesis. *Exp. Biol. Med.* (*Maywood*) **226,** 78–84 CrossRef Medline
48. Eaton, S. (2002) Control of mitochondrial β-oxidation flux. *Prog. Lipid Res.* **41,** 197–239 CrossRef Medline
49. Shoda, J., Oda, K., Suzuki, H., Sugiyama, Y., Ito, K., Cohen, D. E., Feng, L., Kamiya, J., Nimura, Y., Miyazaki, H., Kano, M., Matsuzaki, Y., and Tanaka, N. (2001) Etiologic significance of defects in cholesterol, phospholipid, and bile acid metabolism in the liver of patients with intrahepatic calculi. *Hepatology* **33,** 1194–1205 CrossRef Medline